

CHEMISTRY & SUSTAINABILITY

# CHEM **SUS** CHEM

ENERGY & MATERIALS

## Accepted Article

**Title:** Simultaneous upgrading of furanics and phenolics via hydroxyalkylation/aldol condensation reactions

**Authors:** TUONG V BUI, Tawan Sooknoi, and Daniel E. Resasco

This manuscript has been accepted after peer review and appears as an Accepted Article online prior to editing, proofing, and formal publication of the final Version of Record (VoR). This work is currently citable by using the Digital Object Identifier (DOI) given below. The VoR will be published online in Early View as soon as possible and may be different to this Accepted Article as a result of editing. Readers should obtain the VoR from the journal website shown below when it is published to ensure accuracy of information. The authors are responsible for the content of this Accepted Article.

**To be cited as:** *ChemSusChem* 10.1002/cssc.201601251

**Link to VoR:** <http://dx.doi.org/10.1002/cssc.201601251>

WILEY-VCH

[www.chemsuschem.org](http://www.chemsuschem.org)

A Journal of



# Simultaneous upgrading of furanics and phenolics via hydroxyalkylation/aldol condensation reactions

Tuong V. Bui, Tawan Sooknoi, Daniel E. Resasco\*

*School of Chemical, Biological and Materials Engineering*

*University of Oklahoma*

*100 E. Boyd St., Norman, OK 73019, USA*

## Abstract:

The simultaneous conversion of cyclopentanone and m-cresol has been investigated on a series of solid acid catalysts. Both compounds are representative of biomass-derived streams. Cyclopentanone can be readily obtained from sugar-derived furfurals via Piancatelli rearrangement under reducing conditions. Cresol represents the family of phenolics, typically obtained from the depolymerization of lignin. In the first biomass conversion strategy proposed here, furfural is converted in high yields and selectivity to cyclopentanone (CPO) over metal catalysts such as Pd-Fe/SiO<sub>2</sub> catalyst at 600 psia H<sub>2</sub> and 150°C. Subsequently, CPO and cresol are further converted via acid-catalyzed hydroxyalkylation. This C-C coupling reaction may be used to generate products in the molecular weight range that is appropriate for transportation fuels. Since molecules beyond this range may be undesirable for fuel production, a catalyst with suitable porous structure may be advantageous for controlling the product distribution in the desirable range. In fact, when Amberlyst resins were used as a catalyst, C<sub>12</sub>-C<sub>24</sub> products were obtained, whereas when zeolites with smaller pore sizes were used, they selectively produced C<sub>10</sub> products. Alternatively, CPO can undergo the acid-catalyzed self-aldol condensation to form C<sub>10</sub> bicyclic adducts. As an illustration of the potential of practical implementation of this strategy for biofuel production, the long chain oxygenates obtained from hydroxyalkylation/aldol condensation were successfully upgraded via hydrodeoxygenation to a mixture of linear alkanes and saturated cyclic hydrocarbons, which in practice would be direct drop-in components for transportation fuels. Aqueous acidic environments, typically encountered during the liquid-phase upgrading of bio-oils would inhibit the efficiency of base-catalyzed process. Therefore, the proposed acid-catalyzed upgrading strategy is advantageous in terms of process simplicity for biomass conversion.

## Introduction

Fossil sources exhibit undoubted technological and economical advantages for production of chemicals and transportation fuels. However, emission of greenhouse gases (CO<sub>2</sub> and CH<sub>4</sub>) is an issue of critical concern regarding global warming and climate change. This concern has led to increased research efforts with the goal of commercializing fuels and chemicals from biomass sources that would greatly reduce the carbon footprint. However, techno-economic evaluations indicate that immediate implementation is not possible. The great variety of oxygenated compounds with incompatible chemistries makes a single-stage

upgrading practically impossible. Therefore, greater efforts are needed to help in the development of more efficient biomass upgrading technologies with a number of unit operations that make the process economically feasible. Although several strategies have been investigated to process vapors and liquids derived from biomass pyrolysis, finding efficient processes that can be techno-economically attractive has been challenging [1]. The direct catalytic hydrotreating of condensed bio-oil faces major problems [2, 3], including low yields of liquids in the fuel range and high hydrogen pressures, which complicates their integration with a pyrolysis system [4]. Incorporation of pre-hydrogenated bio-oils into conventional petroleum feedstocks in refinery operations, such as the fluidized catalytic cracking (FCC) and hydrotreating units [5, 6] have also shown technical

Corresponding Author: Prof. Dr. D. E Resasco  
E-mail: ouresasco@gmail.com

impediments that may obstruct their implementation in commercial processes. Some important advances have been made in the upgrading of pyrolysis vapors that leads to enhanced stability of the condensed liquid by forming C-C bonds before adjusting the oxygen content [7, 8].

In the last few years, we have investigated possible conversion paths for separated vapors and liquids obtained from fractionation of bio-oil via step-wise condensation of pyrolysis vapors [9, 10] as well as multistage pyrolysis process [11, 12]. The core of this approach is to carry out the sequence of thermal treatments by heating the biomass at increasing temperatures so that the bio-oil is fractionated into different streams, each one enriched in either light oxygenates, or sugar-derived compounds, or phenolics-derived compounds, respectively [11, 12]. Accordingly, by segregating each specific group of functional molecules in a separate fraction, a combined catalytic upgrading strategy can be developed more selectively and effectively, exploiting the different chemistries of each fraction and optimizing the upgrading instead of a single hydrotreating step for the full bio-oil [13-15].

The fraction of light-oxygenates is rich in acetic acid, acetol, and acetaldehyde. We have previously proposed [14] that they could undergo ketonization to produce acetone, which in turn could be coupled with furfural, an abundant component in the sugar-derived stream, to produce C<sub>8</sub>-C<sub>13</sub> oxygenates over basic catalysts [16, 17]. Alternatively, instead of directly condensing with acetone, furfural can also be pre-stabilized into key intermediates to diminish carbon losses and humins formation, a major cause of catalyst deactivation. The intermediate products are still functional, so they can be further upgraded (C-C bond-chain enlarged) to a wide range of desirable products.

Hydrogenation-decarbonylation of furfural to furan compounds (i.e., methyl furan, dimethyl furan) [18, 19], ring rearrangement of furfural to cyclopentanone (CPO) via Piancatelli reaction [20-22], or oxidation of furfural to carboxylic acids [23, 24] are outstanding examples of furfural conversion into more stable forms that have been recently reported in the literature. In the so-called Sylvan process, methyl furan is condensed with different types of carbonyl compounds, such as acetone, butanal, or furfural [25, 26] to elongate the carbon chain and bring the products to the fuel range. Dimethyl furan can also be coupled with ethylene via Diels-Alder reaction to produce valuable aromatics such as p-xylene [27]. Specific

strategies for upgrading biomass-derived furanics via C-C coupling reaction have been analyzed in our recent review [28].

Interestingly, Hronec et al. [29, 30] have shown that the Piancatelli ring rearrangement in reducing condition is also a promising route to stabilize furfural into cyclopentanone. This is a remarkable pathway, because the O heteroatom is removed from the ring, producing CPO a useful chemical and potential building block for C-C coupling reactions [29]. Although the Piancatelli ring rearrangement of furfuryl alcohol readily occurs in hot liquid water without the need of an additional catalyst, hydrogenation is required to first hydrogenate the CO group in furfural, as well as the resulting C=C double bond after the ring closure to obtain CPO. For this reaction, noble metal catalysts such as Pt, Pd, Ru, Ir as well as inexpensive metals such as Ni, Cu have been used in the conversion of furfural in aqueous phase under H<sub>2</sub> pressure [31, 32]. For example, over 75% yield of CPO has been reported over Pt/C or Ni-CNTs [22, 33]. High selectivity toward cyclopentanone is a definite techno-economic advantage of this approach compared to other upgrading strategies. For the Piancatelli rearrangement, the presence of liquid water plays a crucial role in the reaction [20, 22, 30]. Moreover, the presence of acetic acid in the reaction mixture provides a positive effect on the yield of the desired products [29]. That is, components that are naturally present in biomass-derived streams, i.e., aqueous solutions with high acidity, favor the occurrence of this reaction. Not only CPO is a very convenient building block for carbon retention in the liquid fuel range, but reaching high conversions of furanics to this single molecule greatly reduces catalyst deactivation by avoiding the typical resinification of furfurals to humins. From all of this, we propose that the path of furanics to cyclopentanone is a very effective strategy for upgrading of furfural-rich streams [28].

The phenolics fraction can also be used to effectively incorporate into the fuel range those oxygenates that are too small to be directly hydrotreated. That is, converting C<sub>2</sub>-C<sub>4</sub> oxygenates to alcohols greatly facilitates their incorporation via alkylation. For example, iso-propanol, obtained from hydrogenation of acetone, can produce hydrocarbons in a molecular weight range suitable for the gasoline/diesel pool. Corma et al. [25, 34, 35] have pointed out the feasibility of forming C-C bonds between carbonyl compounds with other organic molecules whenever their electron-density is high enough to promote the electrophilic-attack of the oxonium ion

generated by the protonation of the carbonyl group. Phenolics compounds such as m-cresol and guaiacol, abundant species in biomass pyrolysis vapors, are suitable candidates as hydroxyalkylation aromatic substrates. In fact, several studies have reported successful examples of hydroxyalkylation in systems comprising acetaldehyde/p-cresol [36], acetaldehyde/phenol [37], formaldehyde/guaiacol [38], acetaldehyde/o-xylene [39], aldehyde/benzene derivatives [40, 41], acetone / phenol [42], benzaldehyde/benzene derivatives [43], paraformaldehyde / anisole [44], formaldehyde/benzene [45], formaldehyde / phenol [46] over acid-functionalized solids, such as Amberlyst acidic resin and acidic zeolites to produce crucial platforms for the chemical industry. For example, Rode et al. [47] have reported 80-95% yields of coupling products from the reaction of acetaldehyde/p-cresol over H $\beta$  and bentonite clay catalysts impregnated with dodecatungstophosphoric acid.

In this contribution, we propose a novel approach for the simultaneous upgrading of furfural and m-cresol, two model compounds that represent two streams of sequential biomass thermal treatment at moderate and high temperatures. In this strategy, furfural is first pre-stabilized as cyclopentanone via the Piancatelli rearrangement/hydrogenation process [22, 48]. This intermediate product is then used to hydroxyalkylate m-cresol and generate C<sub>10</sub>-C<sub>24</sub> oxygenates, a suitable range for transportation fuel precursors.

## Results and Discussion

### 1. Hydroxyalkylation of m-cresol/cyclopentanone

#### a) Product distribution over solid acid Amberlyst 15:

The hydroxyalkylation of m-cresol and CPO yields various cyclopentyl-substituted cresol compounds including (3), (4), (5) and (6) (HAA products) as shown in path B **Scheme 1**. Two products from self-aldol condensation of cyclopentanone including (1) and (2) (AC products) were also observed, as shown in path A. In most cases, the formation of product (2) is negligible compared to that of the other products; therefore, in most runs, product (1) is the only representative of the self-aldol condensation reaction.

**Figure 1** shows the reaction data obtained after 2 h in a batch reactor on Amberlyst 15 in the temperature range 65-145°C at a 2:1 m-cresol/CPO molar feed ratio. The results demonstrate that the acid resin displays an acceptable activity,

with conversion increasing from 8 to 38% as the temperature increases, keeping a good carbon balance. For instance, 13% CPO conversion was obtained at 100°C, with 40% selectivity to AC products, 60% selectivity to HAA products and a carbon balance of 98%. Higher temperatures favor the formation of monomer and dimer coupling products (1, 3, 4, and 5). Above 120°C, the decomposition of the trimer (6) becomes evident and undesired reactions start to occur. For example, at 145°C, the carbon balance dropped from almost 100 to 83 %, most probably due to polymerization as indicated by the change in color of the solution. One problem associated with the use of a resin catalyst like Amberlyst 15 is the decomposition of the polymeric matrix that may become significant as temperature increases.

The acid-catalyzed formation of AC products is in itself an interesting outcome of the study since the aldol condensation of cyclopentanone has been typically reported over basic catalysts, such as MgO, KF/Al<sub>2</sub>O<sub>3</sub>, CaO-CeO<sub>2</sub>, CaO, magnesium–aluminum hydrotalcites (MgAl-HT) and lithium–aluminum hydrotalcites (LiAl-HT) [48], or even in NaOH solutions [30]. While it is widely known that the aldol condensation can be catalyzed by both bases and acids, the latter has seldom been reported for cyclopentanone. Zou *et al.* [49] reported the self-aldol condensation of cyclopentanone and cyclohexanone in glass reactor over MOF-encapsulating phosphotungstic, Amberlyst 15 and HZSM-5 materials. The reaction was conducted at 130°C in pure cyclic ketone for 48h and moderate conversion of the ketones could be obtained. However, no information related to carbon balance was reported.

In this work, the experiments were conducted in a Parr reactor in more controlled and quantitative ways than previous studies with shorter reaction times and direct measurement of the carbon balance. The results summarized in **Figure 2** confirm that solid acids such as Amberlyst 15 are capable of producing acceptable yields of AC products (1+2). The yield of the monomer (1) increases over time, reaching 16% after 6 hrs of reaction. The amount of dimer product (2) is very small, reaching only about 1% yield. Excellent carbon balances of 94-97% were observed in both cases. Although the reaction conditions and catalyst formulations will need to be optimized to enhance the yield to coupling compounds, these preliminary results are promising enough to be considered an interesting approach for biomass conversion, particularly since the acidic environment is



commonly found in bio-oil upgrading. The high content of water in real pyrolysis mixtures would require to operate in biphasic system [50]. Implementation of the concepts derived from model compound studies in the separation and conversion of bio-oil to fuel may demonstrate the advantage of using solid emulsifier materials such as hydrophobized zeolites [51, 52] nanotubes, and other amphiphilic catalysts that stabilize emulsions [53] to achieve maximized adducts yields for the reaction.

#### b) *Comparison of different solid acid catalysts:*

Based on these observations, several solid catalysts with different characteristics, including a resin with higher acid density (Amberlyst 36), a microporous zeolite (H $\beta$ ), and a mesoporous acid catalyst (SiO<sub>2</sub>-Al<sub>2</sub>O<sub>3</sub>) were investigated and compared to a homogeneous catalyst, para-toluene sulfuric acid (p-TSA) to explore the effect of catalyst topology and acidity. To make a proper comparison of selectivity, we adjusted the reaction temperature to reach an overall CPO conversion of about 15 %. Specifically, the activity comparison was made at 100°C for Amberlyst and p-TSA, and at 250°C for H $\beta$ , SiO<sub>2</sub>-Al<sub>2</sub>O<sub>3</sub>. The results are summarized in **Table 1** and **Figure 3**. Amberlyst 36 shows an analogous behavior to Amberlyst 15, reaching 15% CPO conversion with selectivities of 38% and 62% for AC and HAA products, respectively. Interestingly, while (at 100°C) Amberlyst resins catalyzed the generation of both AC

and HAA, the zeolite H $\beta$  and amorphous SiO<sub>2</sub>-Al<sub>2</sub>O<sub>3</sub> yielded only AC products (at 250°C).

It is possible that the drop in HAA selectivity might be due to different steric constraints in the catalysts. For instance, Amberlyst resins have large cavities that may allow the formation and desorption of the relatively large HAA products (see example of products 3, 4, 5 and 6 in **Scheme 1**). By contrast, the more constrained Zeolite H $\beta$  may only allow the smaller AC products (93% selectivity) leave the zeolite, while the HAA, if formed will remain trapped inside the microporous structure. It is suggestive that the homogeneous p-TSA exhibits a higher selectivity to large HAA products (3 + 4 + 5 + 6) (**Figure 3**) in comparison to the behavior of solid catalysts. More specifically, at comparable CPO conversion (15-20%) the yields of 3, 4, 5 and 6 were 2.4%, 1.7%, 0.16% and 0.4% on Amberlyst 36 while they are much higher, reaching 5.2%, 1.3%, 1.8% and 12.4%, respectively with the homogeneous catalyst p-TSA.

To check the effect of reaction temperature to the product distribution, reaction runs were conducted on zeolite H $\beta$  at different temperatures (100-250°C). As shown in the **Table 1**, the selectivity on this zeolite did vary with temperature. Higher selectivity toward HAA is favorable as the temperature decreases. This observation agrees with those obtained from homogeneous catalysts in which low temperature favors the formation of HAA products rather than AC products.

**Table 1.** Activity and Average pore size of screened catalysts

| Catalyst  | T, °C | Conversion, % | Selectivity, % |      | Yield, % |       | Acid density, mmol/g <sub>cat</sub> | Conversion per site (mol.L <sup>-1</sup> .mmol <sub>acid</sub> <sup>-1</sup> ) | Carbon balance, % | Average pore size, nm |
|---|-------|---------------|----------------|------|----------|-------|-------------------------------------|--|-------------------|-----------------------|
|   |       |               | AC             | HAA  | AC       | HAA   |                                     |  |                   |                       |
| p-TSAA  | 100   | 20            | 9.3            | 90.7 | 2.9      | 27.5  | 5.8 <sup>c</sup>                    | 1.3  | 97                | -                     |
| Amberlyst 15 <sup>a</sup>                                     | 100   | 12.8          | 39.6           | 60.4 | 3        | 3.5   | 4.7 <sup>c</sup>                    | 0.6  | 94                | 29 <sup>c</sup>       |
| Amberlyst 36 <sup>a</sup>                                     | 100   | 15.3          | 38             | 62   | 4.5      | 4.6   | 4.9 <sup>c</sup>                    | 0.7  | 94                | 24 <sup>c</sup>       |
| Zeolite H $\beta$ <sup>b</sup>                                | 100   | 6.8           | -              | -    | -        | -     | 0.75 <sup>d</sup>                   | 2.02   | 90                | 0.6 <sup>f</sup>      |
|   | 120   | 11            | 71.1           | 28.9 | 0.2      | 0.045 |                                     | 3.38   | 93                |                       |
|   | 200   | 11.7          | 85             | 15   | 2.9      | 0.2   |                                     | 3.48   | 92                |                       |
|   | 250   | 16.3          | 93             | 7    | 11       | 0.5   |                                     | 4.86   | 94                |                       |
| SiO <sub>2</sub> -Al <sub>2</sub> O <sub>3</sub> <sup>b</sup> | 100   | 0.76          | -              | -    | -        | -     | 0.53 <sup>e</sup>                   | 0.32   | 98                | 4.8 <sup>g</sup>      |
|   | 150   | 1.14          | -              | -    | -        | -     |                                     | 0.48   | 99                |                       |
|   | 200   | 5.42          | 99             | 1    | 0.9      | 0.004 |                                     | 2.29   | 95                |                       |
|   | 250   | 17            | 98             | 2    | 10.4     | 0.1   |                                     | 7.26   | 96                |                       |
|   | 280   | 33.8          | 95             | 5    | 21.6     | 0.7   |                                     | 14.3   | 85                |                       |

<sup>a</sup>Glass reactor; <sup>b</sup>Parr reactor; <sup>c</sup>reported by manufacturer; <sup>d</sup>measured by TPD-isopropyl amine <sup>e</sup>ref [54] <sup>f</sup>ref. [55], <sup>g</sup>measured by BET-N<sub>2</sub> ads./des.

However, at this point, it can be concluded that although the temperature can change product distribution, the porous characteristic of solid acid catalysts is the dominant factor that makes AC products dominant (i.e., over 70% sel. at 120°C). At 100°C, no adducts were observed. In the case of SiO<sub>2</sub>-Al<sub>2</sub>O<sub>3</sub>, the same analysis was conducted with temperature range from 100 to 280°C. Interestingly, high selectivity towards AC is observed in all cases. With a large pore size, (average 4.8 nm) and rather slow reactions, one would not expect internal mass transfer limitations on this mesoporous material. As shown in **Figure 4a**, the variation of overall CPO conversion as a function of temperature indicates an apparent activation energy of about 50 kJ/mol, while on the H $\beta$  zeolite, which is clearly affected by mass transfer limitations, the apparent activation energy is only 4.5 kJ/mol. Moreover, when the product yields are used for the Arrhenius plot (**Figure 4b**), apparent activation energy values of about 90 and 140 kJ/mol are obtained for AC and HAA formation, respectively.

The low activity exhibited by the amorphous silica-alumina catalyst towards formation of HAA products could be due to the relatively weak acid strength of this material. Indeed, calorimetry measurements of ammonia adsorption on SiO<sub>2</sub>-Al<sub>2</sub>O<sub>3</sub> give evidence of much lower density of strong acid sites than Amberlyst or any zeolite [56, 57]. Therefore, the acid strength of the mesoporous silica-alumina might not be high enough for catalyzing HAA reaction. That is, only materials with strong acidity and large pore structure could be effective catalysts for the HAA reaction.

To gain a deeper understanding of the pathway for HAA product formation on zeolite H $\beta$ , several separate runs were conducted at 250°C with varying amounts of catalyst. As seen in **Figure 5a, b** the yields of HAA and AC products uniformly increase with the amount of catalyst, as expected. At the same time, it is observed that while the selectivity to product (3) dominates at low yields (at the lowest catalyst mass) the selectivity to products (4) and (5) increased with overall conversion which demonstrates the expected series/parallel sequence for this reaction, i.e., CPO  $\rightarrow$  (3); followed by (3)  $\rightarrow$  (4) or (3)  $\rightarrow$  (5). In this case, no traces of product (6) were observed.

Another series of independent runs was conducted, keeping the catalyst mass constant while varying temperatures. As shown in **Figure 5c**, contrary to the behavior of Amberlyst 15

and 36, which were able to achieve measureable yields (7-9%) at low temperatures (100-120°C), the H $\beta$  catalyst only generated small amounts of condensation products at these temperatures (traces of AC and HAA products were detected). It is conceivable that the diffusion of these large products out of the micro-porous structure is greatly hindered at low temperatures in this zeolite, leading to some disappearance of CPO, but without the formation of any noticeable coupling products. **Figure 5d** shows the distribution of HAA products from zeolite H $\beta$  as a function of reaction temperature. At low temperatures (100-120°C), the major product is (5), which is necessarily produced from product (3). By contrast, at higher temperatures, the selectivity towards product (5) decreases while that to (3) increases. Clearly, at high enough temperatures, product (5) begins to decompose via C-C cleavage yielding back product (3). The low selectivity towards product (4) might be due to the higher abundance of m-cresol with respect to CPO (m-cresol/CP feed ratio = 2:1).

In fact, as shown in **Table 1**, the carbon balance is over 90% for all cases. That is, by using a less reactive intermediate such as cyclopentanone, not only the carbon losses can be minimized, but valuable condensation products can be obtained with less humins formation.

c) Effect of temperature on the competition between self-aldol condensation (AC) and hydroxyalkylation (HAA):

The investigated reaction, in fact, is complicated since two possible parallel reactions are taking place at the same time. The relative rate between two pathways depends on factors such as feed ratio, temperature, etc. Moreover, the porous characteristic of each solid catalyst places different influence in the diffusion of formed products and so on the obtained product distribution. A series of experiments was conducted with a homogeneous catalyst (para-toluene sulfuric acid) to get an insight into the nature of this reaction. In this case, there is no possible role of porous cavities affecting the product distribution as in solid acid catalysts. As shown in **Figure 6a**, at low temperatures (e.g., 60°C), hydroxyalkylation products (HAA) dominate, with selectivity above 90%. As temperature increases, the selectivity toward aldol condensation products (AC) slowly increases (up to 150°C) but beyond this temperature, it jumps dramatically from 20% at 200°C to 60% at 250°C. The change of product distribution with increasing temperature in this case might be due to the low stability of the HAA C-C coupling

products (the alcohol) that makes it easily decomposed back to CPO and m-cresol at high temperature (250°C) before dehydration. This results in more abundant AC products at 250°C.

At the lowest temperature, only the C-C coupling monomer (3) is observed in the products. However, at 100°C, the trimer (6) is formed easily, becoming one of the most abundant products and reaching 45% selectivity. As the temperature is further increased, the selectivity to (6) greatly decreases with the other products increasing, even when the reactant conversion remained unchanged. It is clear that (6) starts decomposing back to monomer (3). Indeed, negligible amounts of the trimer (6) are detected at 250°C. Likewise, as shown previously (**Figure 1**), similar decomposition of the trimer (6) is observed over the solid acid Amberlyst 15 at temperatures above 120°C. **Figure 6b** also shows similar trends for the trimers (4) and (5), which initially increase with temperature, but then decrease, reaching a maximum selectivity at 200°C (~20%).

The possible reaction mechanism includes four primary steps: (a) protonation of cyclopentanone on acid sites to form an enolate, (b) C-C coupling of the activated CPO with another CPO or m-cresol to form condensation products (ACol and HAAol), (c) deprotonation, and (d) dehydration of the resulting alcohols to generate the AC and HAA products. It is possible that the rate limiting step for each reaction could be one of those. However, in the presence of acid catalysts the dehydration step is relatively fast. It should be noted that the relative activation energy between each step could be shifted, depending on catalysts with different acid strength. More detailed kinetic and theoretical studies are required on each individual reaction to obtain a more comprehensive understanding of the system.

#### d) *Effect of feed ratio:*

Both AC and HAA can yield products with longer carbon chains, which can subsequently be hydrodeoxygenated to molecules that directly fall in the gasoline/diesel range. In some applications, it may be desirable to produce a narrow molecular weight distribution. In this case, our results show that a narrower molecular weight distribution can indeed be obtained by adjusting the m-cresol/CPO feed ratio. As illustrated in **Figure 7**, as the m-cresol/CPO increases from 2:1 to 5:1, the yield of AC products drops from 4.5% to 1.4% while that of HAA products

increases from 3.7 to 5.4%. Interestingly, when the m-cresol/CPO ratio increases to 7:1, only HAA products are obtained with no traces of AC products.

## 2. Hydrodeoxygenation of coupling products obtained in the first step

Hydrodeoxygenation is the final step after accomplishing the desired molecular weight via C-C coupling. For practical implementation as fuels, the coupling compounds generated from hydroxyalkylation would need to be saturated and deoxygenated to produce alkanes with properties similar to those derived from petroleum energy sources. To demonstrate the sequence, first, the C-C coupling step was carried via HAA reaction on a 3g Amberlyst 36 sample in a Parr reactor (150°C, m-cresol/CPO=2:1, 12h). In this step, the goal is to obtain a reasonable yield of coupling products, which can be used later as feedstock for the HDO upgrading. In this case, 51% CPO conversion with a wide range of long-chain oxygenates was obtained, as shown in **Figure 8**, with (1) and (3) as major products, accounting for 18% and 14% yield, respectively.

To carry out the HDO upgrading step, 2 ml of the liquid product of the previous step was diluted in 118 ml of undecane solvent together with 500 mg of 2% Pd/Al<sub>2</sub>O<sub>3</sub> catalysts. The catalyst was reduced at 150°C for 3 h under 400 psia of H<sub>2</sub>. The HDO run was conducted at 250°C in the batch reactor for 12 h. The most abundant products were cyclopentane and methyl cyclohexane, which come from the hydrogenation/dehydration of CPO and m-cresol. Long-chain hydrocarbon products include fully saturated C<sub>10</sub> alkanes, C<sub>12</sub> cyclic and C<sub>12</sub> alkane products which are generated from the ring opening of the saturated species (1) and hydrogenation of (3), followed by the ring opening, respectively (**Scheme 2** and **Figure 9**). Trace amount of carbon chain longer than 12 was observed, which is probably due to the decomposition of dimer/trimer at the high temperatures and long reaction time used in this experiment. The observed alkanes represent over 39% selectivity of the upgraded liquid. In fact, hydrogenated products derived from m-cresol, such as methylcyclohexane or methylcyclohexanol, also fall into gasoline range (C<sub>7</sub>-C<sub>12</sub>). Therefore, the whole applicable products in the fuel range would account for 90% of the upgraded liquid. More interestingly, the carbon balance for the HAA and HDO steps are 96% and 95%, respectively, resulting in over 90% efficiency for the whole catalytic upgrading process, which starts from CPO and results in with drop-in liquid fuel

products. This promising result illustrates the great potential of this strategy for biomass-derived liquid fuel production.

## Conclusions

The Piancatelli rearrangement of furanic compounds to CPO represents a very attractive biomass upgrading strategy that pre-stabilizes reactive molecules such as furfural into a useful and less reactive ketone. Compared to conventional hydrogenation/hydrogenolysis strategies, this approach demands less energy and less H<sub>2</sub> consumption. In addition, the high water and acid content of bio-oil are in fact favorable for this conversion, which makes the process more appealing in terms of practical implementation. The production of this stable intermediate can be followed by C-C bond formation reactions, such as self-aldol condensation or hydroxyalkylation with phenolics-derived fractions. When the C-C bond forming process is followed by a hydrodeoxygenation step a mixture of C<sub>10</sub>-C<sub>16</sub> hydrocarbons, which are in the gasoline/diesel range can be effectively obtained. For example, when the product stream from the AC/HAA reaction of CPO and m-cresol was followed by HDO on a bifunctional catalyst over 90% efficiency of the whole catalytic upgrading process starting from CPO was demonstrated, which highlights the potential of this strategy for future biofuel applications.

The major obstacle of this approach is that the large organic molecules produced by the HAA reaction are trapped in microporous catalysts, particularly at low temperatures. Thermally stable zeolites that can be operated at higher temperatures show a lower degree of trapping, but the problem still subsists. Further research on acidic materials with hierarchical structures with a proper mesoporous/microporous balance that minimizes the diffusion path of large adducts out of the catalyst cavities would be desirable.

## Experimental Section

The conversion of furfural to cyclopentanone was carried out in a Parr reactor at 150°C, 14-40 bar for 6 hrs in water solvent over 0.15 g 2% Pd-Fe/SiO<sub>2</sub> catalyst, at an initial concentration of furfural of 200 mM. The hydroxyalkylation of m-cresol with cyclopentanone was conducted at atmospheric pressure in a glass reactor in the temperature range 65-140°C,

for 2 hrs in the presence of Amberlyst 15, Amberlyst 36, or p-TSA (Sigma Aldrich) catalysts. Alternatively, the reaction was conducted in a Parr reactor at 100-250°C, under 300 psia N<sub>2</sub> for 2 hrs in the presence of Zeolite H $\beta$  (Zeolyst) or SiO<sub>2</sub>-Al<sub>2</sub>O<sub>3</sub> (Sigma Aldrich). In all cases, the amount of catalyst used was 0.15 g and the feed was either pure CPO or m-cresol/CPO mixtures. The effect of m-cresol/CPO ratio (2:1, 5:1, and 7:1) on the product distribution was examined in the Parr reactor at 120°C, 300 psia N<sub>2</sub> for 2 hrs in the presence of 1 g Amberlyst 15 in decalin solvent. The aldol condensation of cyclopentanone was examined in Parr reactor at 100°C and 300 psia N<sub>2</sub> for 2 and 6 hrs. 0.5M of CPO in decalin solvent over 1 g Amberlyst 15.

The product mixture was analyzed by Shimadzu QP2010S gas chromatograph/mass spectrometer (GC-MS) and quantified by GC-FID Agilent 6890 equipped with a flame ionization detector for quantification. Both GC's were equipped with a Zebron ZB-1701 column with dimensions of 60m x 0.25 mm x 0.25  $\mu$ m.

The conversion (X), yield and selectivity were calculated as:

$$X = \frac{C_{CPO-in} - C_{CPO-out}}{C_{CPO-in}} ; \quad Y_i = \frac{C_i \times n}{C_{CPO-in}} ;$$

$$S_i = \frac{C_i}{\sum C_i}$$

The carbon balance for the HAA reaction was calculated as:

$$\text{Carbon balance} = \frac{C_{CPO \rightarrow \text{products}} + C_{CPO-out}}{C_{CPO-in}}$$

The carbon balance for the HDO step was calculated as:

$$\text{Carbon balance} = \frac{\sum C_i \times n_{Ci} |_{\text{product}}}{\sum C_i \times n_{Ci} |_{\text{feed}}}$$

where C<sub>CPO</sub>(in, out): Concentration of cyclopentanone before and after reaction;

C<sub>i</sub>: Concentration of each product;

n: Number of cyclopentanone molecule in molecular structure of products;

n<sub>Ci</sub>: Number of carbons in molecular structure

## Acknowledgements



The authors thank the Department of Energy for funding the experimental part of this work under grant DE-SC0004600 and the theoretical part under grant DE-EE0006287 of the Bioenergy Technology Office CHASE program.

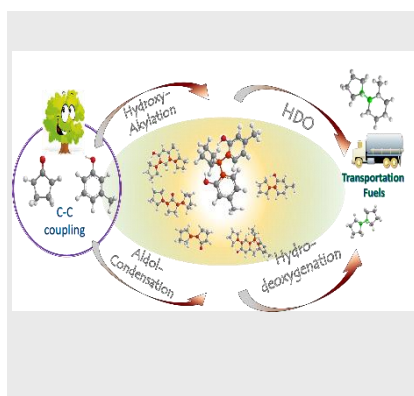
**Keywords:** C-C coupling 1 • hydroxyalkylation 2 • phenolics 3 • cyclopentanone 4 • biofuels 5

Layout 1:

## FULL PAPER

### Table of content

We are here proposing an attractive strategy to effectively upgrade two fractions of torrefraction simultaneously via hydroxyalkylation/aldol condensation reactions. As the results, after HDO processing, saturated alkanes with carbon chain ranging from C<sub>10</sub>-C<sub>16</sub> could be obtained, which could be used as transportation fuel or refinery feed.



Tuong V. Bui, Dr. Tawan Snooknoi,  
Prof. Daniel E. Resasco\*

Page No. – Page No.

**Simultaneous upgrading of furanics  
and phenolics via hydroxyalkylation  
/aldol condensation reactions**

## References:

1. T.N. Pham, D. Shi, and D.E. Resasco, *Evaluating strategies for catalytic upgrading of pyrolysis oil in liquid phase*. Applied Catalysis B: Environmental, 2014. **145**(0): p. 10-23.
2. D.C. Elliott, *Status of Process Development for Pyrolysis of Biomass for Liquid Fuels and Chemicals Production*. Journal Name: International Sustainable Energy Review, 4(2):56-57; Journal Volume: 4; Journal Issue: 2, 2010: p. Medium: X.
3. D.C. Elliott and A. Oasmaa, *Catalytic hydrotreating of black liquor oils*. Energy & Fuels, 1991. **5**(1): p. 102-109.
4. T.L. Marker, L.G. Felix, M.B. Linck, and M.J. Roberts, *Integrated hydropyrolysis and hydroconversion (IH2) for the direct production of gasoline and diesel fuels or blending components from biomass, part 1: Proof of principle testing*. Environmental Progress & Sustainable Energy, 2012. **31**(2): p. 191-199.
5. M.E. Domine, A.C. van Veen, Y. Schuurman, and C. Mirodatos, *Coprocessing of Oxygenated Biomass Compounds and Hydrocarbons for the Production of Sustainable Fuel*. ChemSusChem, 2008. **1**(3): p. 179-181.
6. A.A. Lappas, S. Bezergianni, and I.A. Vasalos, *Production of biofuels via co-processing in conventional refining processes*. Catalysis Today, 2009. **145**(1-2): p. 55-62.
7. H.y. Li, Y.j. Yan, and Z.w. Ren, *Online upgrading of organic vapors from the fast pyrolysis of biomass*. Journal of Fuel Chemistry and Technology, 2008. **36**(6): p. 666-671.
8. C.A. Gaertner, J.C. Serrano-Ruiz, D.J. Braden, and J.A. Dumesic, *Catalytic coupling of carboxylic acids by ketonization as a processing step in biomass conversion*. Journal of Catalysis, 2009. **266**(1): p. 71-78.
9. H. Sui, H. Yang, J. Shao, X. Wang, Y. Li, and H. Chen, *Fractional Condensation of Multicomponent Vapors from Pyrolysis of Cotton Stalk*. Energy & Fuels, 2014. **28**(8): p. 5095-5102.
10. A.S. Pollard, M.R. Rover, and R.C. Brown, *Characterization of bio-oil recovered as stage fractions with unique chemical and physical properties*. Journal of Analytical and Applied Pyrolysis, 2012. **93**(0): p. 129-138.
11. D. Ciolkosz and R. Wallace, *A review of torrefaction for bioenergy feedstock production*. Biofuels, Bioproducts and Biorefining, 2011. **5**(3): p. 317-329.
12. M.J.C. van der Stelt, H. Gerhauser, J.H.A. Kiel, and K.J. Ptasinski, *Biomass upgrading by torrefaction for the production of biofuels: A review*. Biomass and Bioenergy, 2011. **35**(9): p. 3748-3762.
13. P. Zapata, J. Faria, M. Pilar Ruiz, and D. Resasco, *Condensation/Hydrogenation of Biomass-Derived Oxygenates in Water/Oil Emulsions Stabilized by Nanohybrid Catalysts*. Topics in Catalysis, 2012. **55**(1-2): p. 38-52.
14. T.N. Pham, D. Shi, T. Sooknoi, and D.E. Resasco, *Aqueous-phase ketonization of acetic acid over Ru/TiO2/carbon catalysts*. Journal of Catalysis, 2012. **295**: p. 169-178.
15. M.Á. González-Borja and D.E. Resasco, *Reaction pathways in the liquid phase alkylation of biomass-derived phenolic compounds*. AIChE Journal, 2015. **61**(2): p. 598-609.
16. R.M. West, Z.Y. Liu, M. Peter, C.A. Gärtner, and J.A. Dumesic, *Carbon-carbon bond formation for biomass-derived furfurals and ketones by aldol condensation in a biphasic system*. Journal of Molecular Catalysis A: Chemical, 2008. **296**(1-2): p. 18-27.
17. C.J. Barrett, J.N. Chheda, G.W. Huber, and J.A. Dumesic, *Single-reactor process for sequential aldol-condensation and hydrogenation of biomass-derived compounds in water*. Applied Catalysis B: Environmental, 2006. **66**(1-2): p. 111-118.

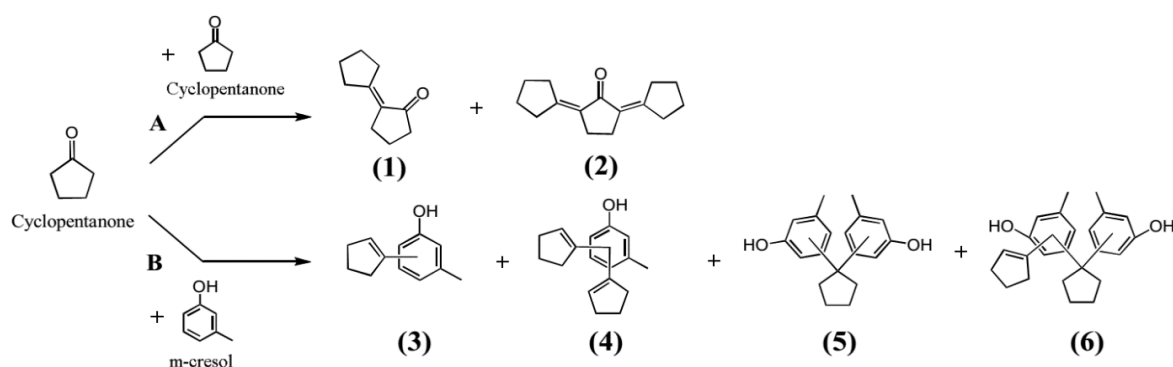
18. H.-Y. Zheng, Y.-L. Zhu, B.-T. Teng, Z.-Q. Bai, C.-H. Zhang, H.-W. Xiang, and Y.-W. Li, *Towards understanding the reaction pathway in vapour phase hydrogenation of furfural to 2-methylfuran*. *Journal of Molecular Catalysis A: Chemical*, 2006. **246**(1–2): p. 18–23.
19. J.Z. Karl, *Methylfuran*, in *Sugar Series*. 2000, Elsevier. p. 229–230.
20. C. Piutti and F. Quartieri, *The Piancatelli Rearrangement: New Applications for an Intriguing Reaction*. *Molecules*, 2013. **18**(10): p. 12290–12312.
21. M. Hronec and K. Fulajtarová, *Selective transformation of furfural to cyclopentanone*. *Catalysis Communications*, 2012. **24**(0): p. 100–104.
22. M. Hronec, K. Fulajtarová, and T. Liptaj, *Effect of catalyst and solvent on the furan ring rearrangement to cyclopentanone*. *Applied Catalysis A: General*, 2012. **437–438**(0): p. 104–111.
23. S. Shi, H. Guo, and G. Yin, *Synthesis of maleic acid from renewable resources: Catalytic oxidation of furfural in liquid media with dioxygen*. *Catalysis Communications*, 2011. **12**(8): p. 731–733.
24. H. Choudhary, S. Nishimura, and K. Ebitani, *Highly Efficient Aqueous Oxidation of Furfural to Succinic Acid Using Reusable Heterogeneous Acid Catalyst with Hydrogen Peroxide*. *Chemistry Letters*, 2012. **41**(4): p. 409–411.
25. A. Corma, O. de la Torre, and M. Renz, *Production of high quality diesel from cellulose and hemicellulose by the Sylvan process: catalysts and process variables*. *Energy & Environmental Science*, 2012. **5**(4): p. 6328–6344.
26. G. Li, N. Li, Z. Wang, C. Li, A. Wang, X. Wang, Y. Cong, and T. Zhang, *Synthesis of High-Quality Diesel with Furfural and 2-Methylfuran from Hemicellulose*. *ChemSusChem*, 2012. **5**(10): p. 1958–1966.
27. C.L. Williams, C.-C. Chang, P. Do, N. Nikbin, S. Caratzoulas, D.G. Vlachos, R.F. Lobo, W. Fan, and P.J. Dauenhauer, *Cycloaddition of Biomass-Derived Furans for Catalytic Production of Renewable p-Xylene*. *ACS Catalysis*, 2012. **2**(6): p. 935–939.
28. T.V. Bui, Crossley S., Resasco, D.E., *C-C coupling for biomass-derived furanics upgrading to chemicals and fuels in Chemicals and Fuels from Bio-Based Building Blocks*. 2016, Wiley-VCH. p. 431–494.
29. M. Hronec, K. Fulajtárova, T. Liptaj, M. Štolcová, N. Prónayová, and T. Soták, *Cyclopentanone: A raw material for production of C15 and C17 fuel precursors*. *Biomass and Bioenergy*, 2014. **63**(0): p. 291–299.
30. Y. Yang, Z. Du, Y. Huang, F. Lu, F. Wang, J. Gao, and J. Xu, *Conversion of furfural into cyclopentanone over Ni-Cu bimetallic catalysts*. *Green Chemistry*, 2013. **15**(7): p. 1932–1940.
31. S. Sitthisa and D. Resasco, *Hydrodeoxygenation of Furfural Over Supported Metal Catalysts: A Comparative Study of Cu, Pd and Ni*. *Catalysis Letters*, 2011. **141**(6): p. 784–791.
32. K. Yan, G. Wu, T. Lafleur, and C. Jarvis, *Production, properties and catalytic hydrogenation of furfural to fuel additives and value-added chemicals*. *Renewable and Sustainable Energy Reviews*, 2014. **38**(0): p. 663–676.
33. M. Zhou, H. Zhu, L. Niu, G. Xiao, and R. Xiao, *Catalytic Hydroprocessing of Furfural to Cyclopentanol Over Ni/CNTs Catalysts: Model Reaction for Upgrading of Bio-oil*. *Catalysis Letters*, 2014. **144**(2): p. 235–241.
34. A. Corma, O. de la Torre, and M. Renz, *High-Quality Diesel from Hexose- and Pentose-Derived Biomass Platform Molecules*. *ChemSusChem*, 2011. **4**(11): p. 1574–1577.
35. A. Corma, O. de la Torre, M. Renz, and N. Vollandier, *Production of High-Quality Diesel from Biomass Waste Products*. *Angewandte Chemie International Edition*, 2011. **50**(10): p. 2375–2378.
36. A.C. Garade, V.R. Mate, and C.V. Rode, *Montmorillonite for selective hydroxyalkylation of p-cresol*. *Applied Clay Science*, 2009. **43**(1): p. 113–117.



37. A.C. Garade, V.S. Kshirsagar, R.B. Mane, A.A. Ghalwadkar, U.D. Joshi, and C.V. Rode, *Acidity tuning of montmorillonite K10 by impregnation with dodecatungstophosphoric acid and hydroxyalkylation of phenol*. *Applied Clay Science*, 2010. **48**(1–2): p. 164–170.
38. M. Bolognini, F. Cavani, L. Dal Pozzo, L. Maselli, F. Zaccarelli, B. Bonelli, M. Armandi, and E. Garrone, *Guaiacol hydroxyalkylation with aqueous formaldehyde: role of surface properties of H-mordenites on catalytic performance*. *Applied Catalysis A: General*, 2004. **272**(1–2): p. 115–124.
39. P. Beltrame, E. Conte, L. Forni, and G. Zuretti, *Screening of solid acid catalysts for the condensation of acetaldehyde with o-xylene*. *Applied Catalysis A: General*, 1995. **128**(1): p. 143–154.
40. M.J. Climent, A. Corma, H. García, S. Iborra, and J. Primo, *Acid zeolites as catalysts in organic reactions: condensation of acetophenone with benzene derivatives*. *Applied Catalysis A: General*, 1995. **130**(1): p. 5–12.
41. M.J. Climent, A. Corma, H. Garcia, and J. Primo, *Zeolites as catalysts in organic reactions: Condensation of aldehydes with benzene derivatives*. *Journal of Catalysis*, 1991. **130**(1): p. 138–146.
42. K. Nowińska and W. Kaleta, *Synthesis of Bisphenol-A over heteropoly compounds encapsulated into mesoporous molecular sieves*. *Applied Catalysis A: General*, 2000. **203**(1): p. 91–100.
43. M. Alvaro, H. García, A. Sanjuán, and M. Esplá, *Hydroxyalkylation of benzene derivatives by benzaldehyde in the presence of acid zeolites*. *Applied Catalysis A: General*, 1998. **175**(1–2): p. 105–112.
44. M. Álvaro, D. Das, M. Cano, and H. Garcia, *Friedel–Crafts hydroxyalkylation: reaction of anisole with paraformaldehyde catalyzed by zeolites in supercritical CO<sub>2</sub>*. *Journal of Catalysis*, 2003. **219**(2): p. 464–468.
45. M.J. Climent, A. Corma, H. García, and J. Primo, *Zeolites in organic reactions: Condensation of formaldehyde with benzene in the presence of HY zeolites*. *Applied Catalysis*, 1989. **51**(1): p. 113–125.
46. Y. Tan, Y. Li, Y. Wei, Z. Wu, J. Yan, L. Pan, and Y. Liu, *The hydroxyalkylation of phenol with formaldehyde over mesoporous M(Al, Zr, Al–Zr)-SBA-15 catalysts: The effect on the isomer distribution of bisphenol F*. *Catalysis Communications*, 2015. **67**: p. 21–25.
47. A.C. Garade, V.S. Kshirsagar, A. Jha, and C.V. Rode, *Structure–activity studies of dodecatungstophosphoric acid impregnated bentonite clay catalyst in hydroxyalkylation of p-cresol*. *Catalysis Communications*, 2010. **11**(11): p. 942–945.
48. J. Yang, N. Li, G. Li, W. Wang, A. Wang, X. Wang, Y. Cong, and T. Zhang, *Synthesis of renewable high-density fuels using cyclopentanone derived from lignocellulose*. *Chemical Communications*, 2014. **50**(20): p. 2572–2574.
49. Q. Deng, G. Nie, L. Pan, J.-J. Zou, X. Zhang, and L. Wang, *Highly selective self-condensation of cyclic ketones using MOF-encapsulating phosphotungstic acid for renewable high-density fuel*. *Green Chemistry*, 2015. **17**(8): p. 4473–4481.
50. D.E. Resasco and S.P. Crossley, *Implementation of concepts derived from model compound studies in the separation and conversion of bio-oil to fuel*. *Catalysis Today*, 2015. **257**, Part 2: p. 185–199.
51. P.A. Zapata, Y. Huang, M.A. Gonzalez-Borja, and D.E. Resasco, *Silylated hydrophobic zeolites with enhanced tolerance to hot liquid water*. *Journal of Catalysis*, 2013. **308**: p. 82–97.
52. P.A. Zapata, J. Faria, M.P. Ruiz, R.E. Jentoft, and D.E. Resasco, *Hydrophobic Zeolites for Biofuel Upgrading Reactions at the Liquid–Liquid Interface in Water/Oil Emulsions*. *Journal of the American Chemical Society*, 2012. **134**(20): p. 8570–8578.
53. D.E. Resasco, *Carbon nanohybrids used as catalysts and emulsifiers for reactions in biphasic aqueous/organic systems*. *Chinese Journal of Catalysis*, 2014. **35**(6): p. 798–806.

- 
- 1 54. T. Masuda, H. Taniguchi, K. Tsutsumi, and H. Takahashi, *Differential Heat of Adsorption of*  
2 *Ammonia on Hydrothermally Treated Solid Acid Catalysts and Their Catalytic Activity*. Journal  
3 of The Japan Petroleum Institute, 1979. **22**(2): p. 67-72.
- 4 55. J. Jae, G.A. Tompsett, A.J. Foster, K.D. Hammond, S.M. Auerbach, R.F. Lobo, and G.W.  
5 Huber, *Investigation into the shape selectivity of zeolite catalysts for biomass conversion*.  
6 Journal of Catalysis, 2011. **279**(2): p. 257-268.
- 7 56. P.F. Siril, H.E. Cross, and D.R. Brown, *New polystyrene sulfonic acid resin catalysts with*  
8 *enhanced acidic and catalytic properties*. Journal of Molecular Catalysis A: Chemical, 2008.  
9 **279**(1): p. 63-68.
- 10 57. M. Tatsuo, T. Hitofumi, T. Kazuo, and T. Hiroshi, *Direct Measurement of Interaction Energy*  
11 *between Solids and Gases. II. Microcalorimetric Studies on the Surface Acidity and Acid*  
12 *Strength Distribution of Solid Acid Catalysts*. Bulletin of the Chemical Society of Japan, 1978.  
13 **51**(7): p. 1965-1969.
- 14  
15  
16  
17  
18  
19  
20  
21  
22  
23  
24  
25  
26  
27  
28  
29  
30  
31  
32  
33  
34  
35  
36  
37  
38  
39  
40  
41  
42  
43  
44  
45  
46  
47  
48  
49  
50  
51  
52  
53  
54  
55  
56  
57  
58  
59  
60  
61  
62  
63  
64  
65
-

## Figures and Schemes



**Scheme 1.** Products from hydroxyalkylation of m-cresol and cyclopentanone

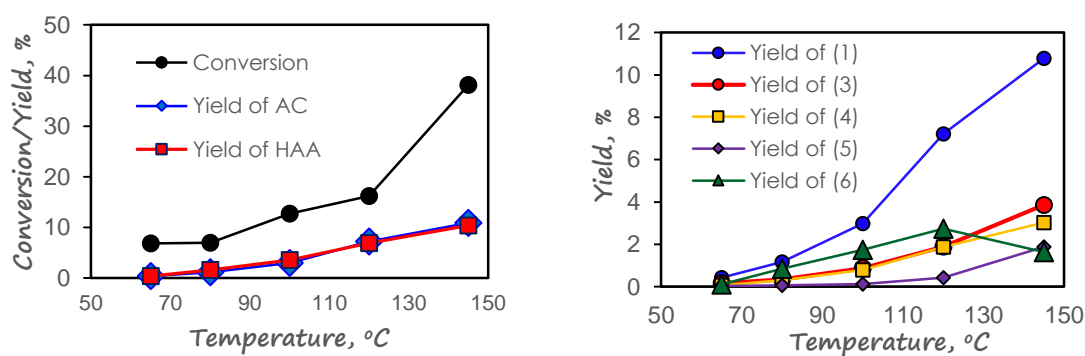


**Figure 1.** Catalytic performance of Amberlyst 15 at different temperatures. Product (1) – (6) are presented in Scheme 1

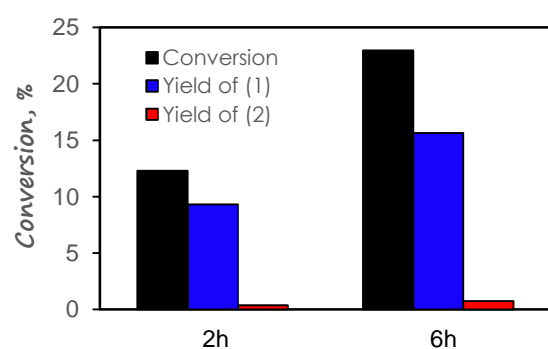


**Figure 2.** The acid-catalyzed aldol condensation of cyclopentanone over Amberlyst 15 (Parr reactor at 100°C and 300 psia N<sub>2</sub> for 2 and 6 hrs in decalin solvent over 1 g Amberlyst 15.)

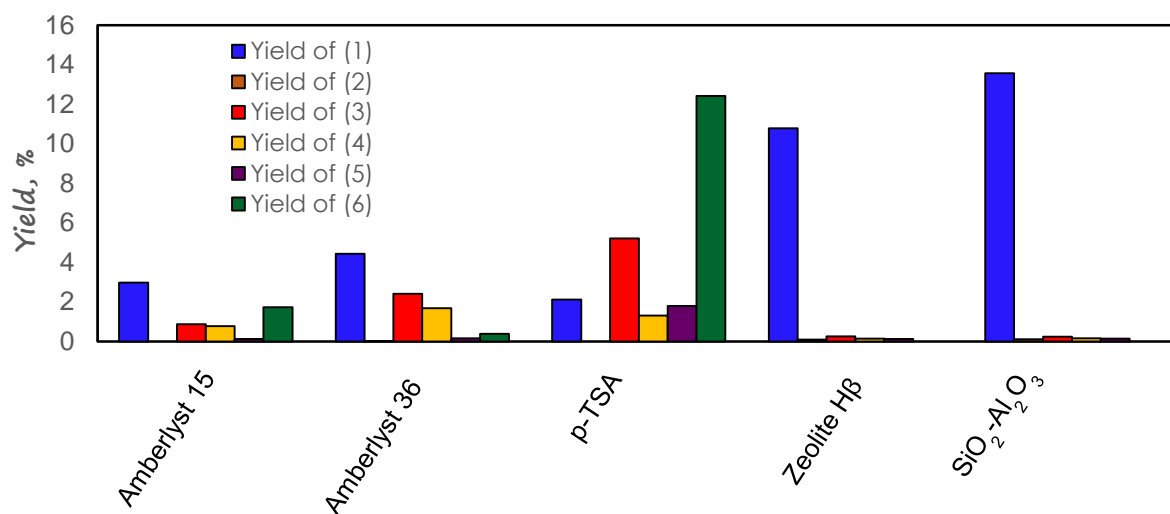


Figure 3. Yield of coupling products from different catalysts at comparable CPO conversion

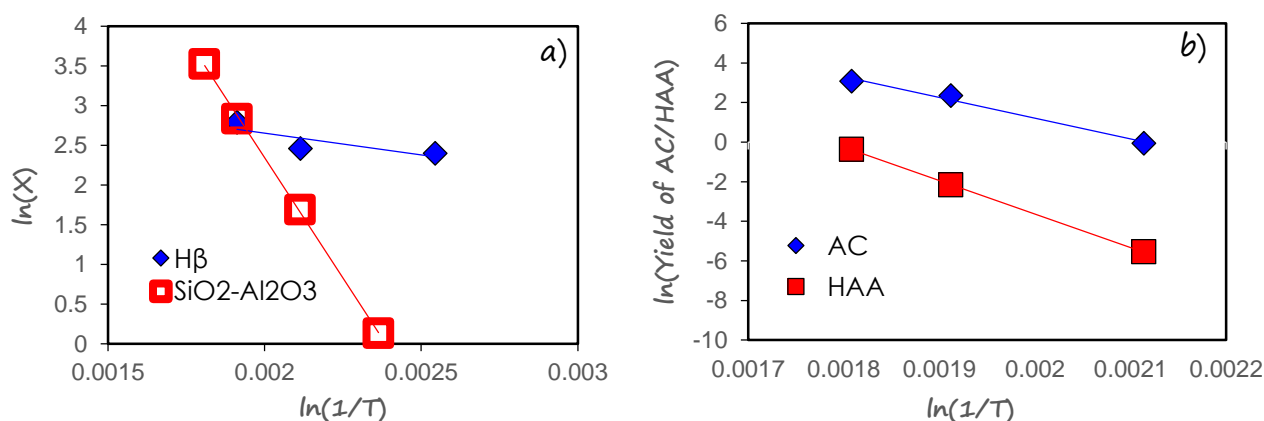
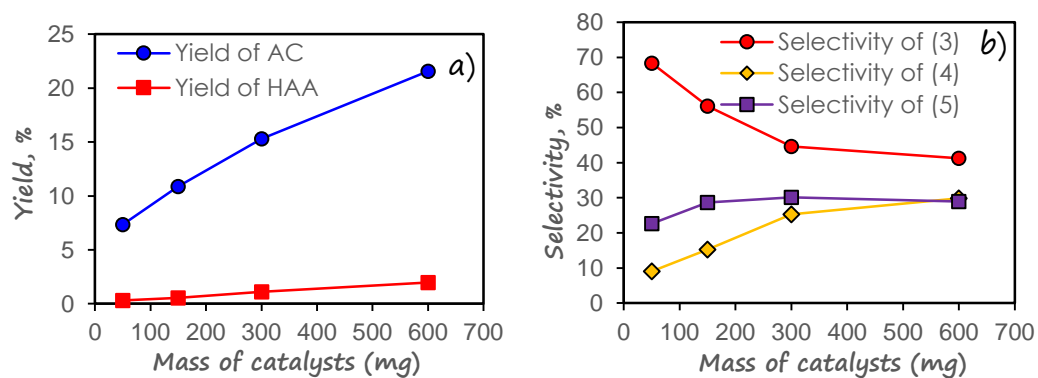
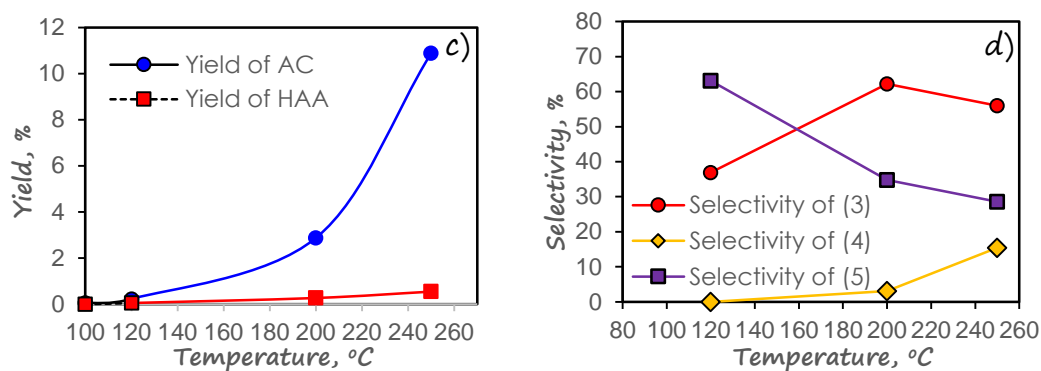


Figure 4. Arrhenius plots for a) overall CPO conversion over Hβ and SiO<sub>2</sub>-Al<sub>2</sub>O<sub>3</sub>; and b) Yield of AC and HAA products over SiO<sub>2</sub>-Al<sub>2</sub>O<sub>3</sub>.







**Figure 5.** a) Yield of AC, HAA products and b) Distribution of HAA products at different mass of catalysts c) Yield of AC and HAA products and d) Distribution of HAA products at different temperatures

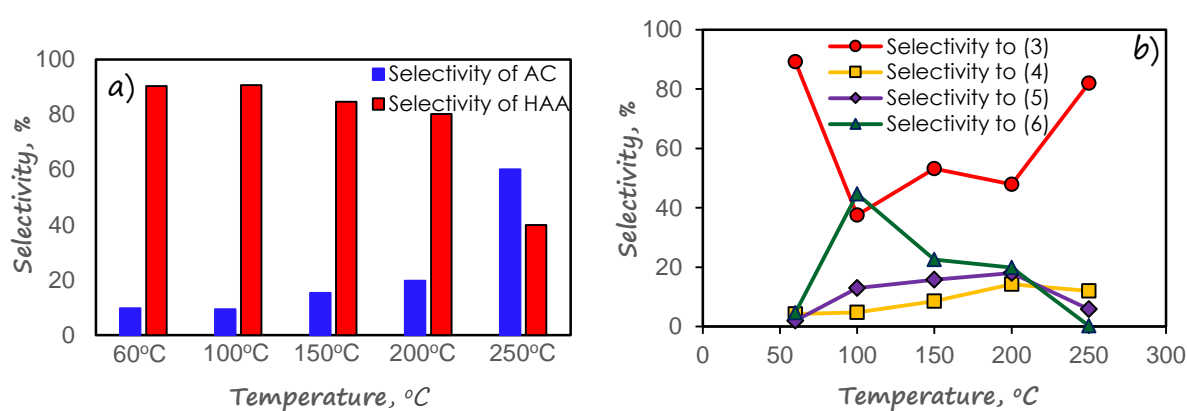


**Figure 6.** a) Selectivity of aldol condensation and hydroxyalkylation products (AC and HAA) at different temperatures (Reaction condition: m-cresol/cyclopentanone=2/1, Parr reaction, reaction volume 120ml, the conversions at 60°C, 100°C, 150°C, 200°C, 250°C are 20%, 20%, 23%, 21%, 20%, respectively) b) Selectivity of hydroxyalkylation products at different temperatures

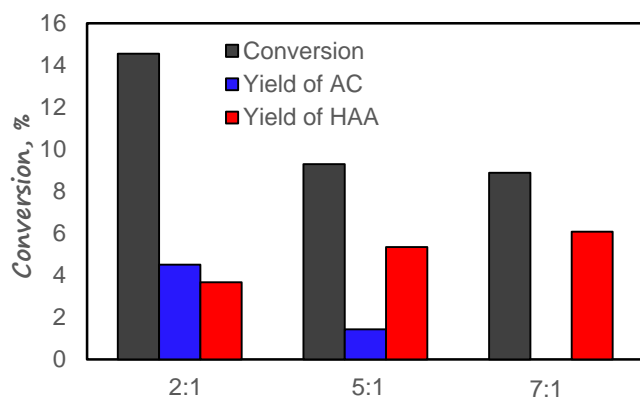


**Figure 7.** The distribution of AC and HAA products at different m-cresol/CPO ratios over Amberlyst 15 (Parr reactor at 120°C, 300 psia N<sub>2</sub> for 2 hrs in the presence of 1 g Amberlyst 15 in decalin solvent)

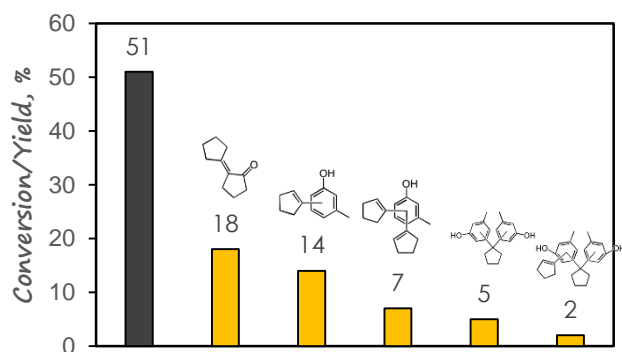
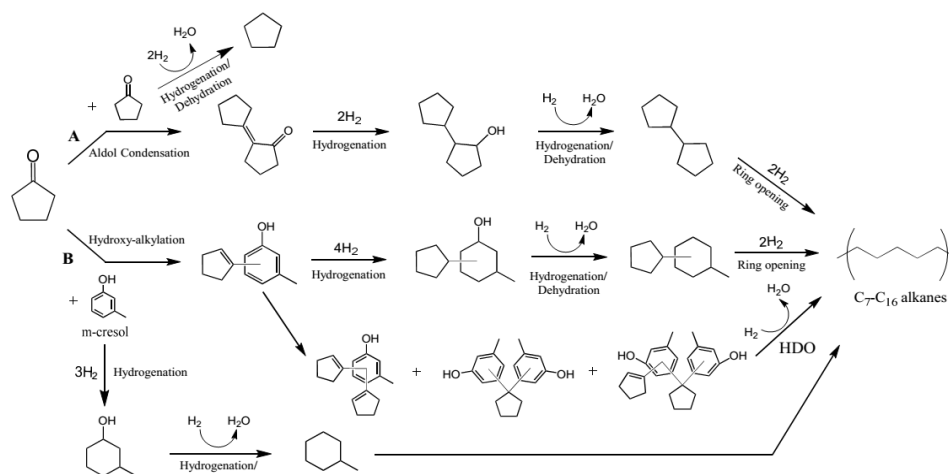


**Figure 8.** Conversion/Yield of HAA reaction between CPO and m-cresol (dash-black bar is the conversion of CPO, yellow bars are the yield of each product)

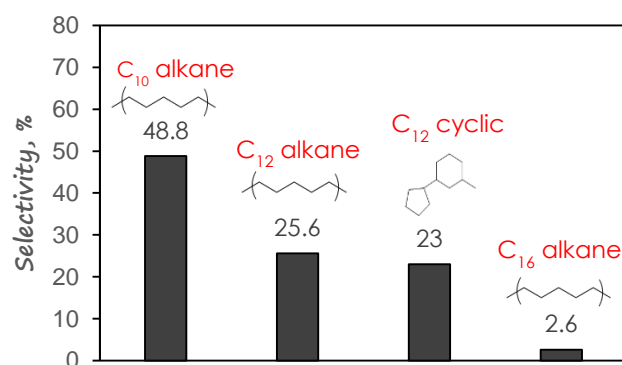


**Figure 9.** Selectivity of each saturated products in HDO upgraded liquid

## Graphical abstract

